

# A laser plasma soliton fusion scheme

Pisin Chen<sup>a,b,c</sup>\*, Yung-Kun Liu<sup>a,b</sup>† and Gerard Mourou<sup>d‡</sup>

<sup>a</sup>*Leung Center for Cosmology and Particle Astrophysics,  
National Taiwan University, Taipei 10617, Taiwan*

<sup>b</sup>*Department of Physics, National Taiwan University, Taipei 10617, Taiwan*

<sup>c</sup>*Graduate Institute of Astrophysics, National Taiwan University, Taipei 10617, Taiwan and*

<sup>d</sup>*International Center for Zetta-Exawatt Science and Technology,  
École Polytechnique, Palaiseau Cedex 91128, France*

We introduce a novel fusion scheme enabled by laser-plasma solitons, which promises to overcome several fundamental obstructions to reaching the breakeven condition. For concreteness, we invoke deuterium-tritium (DT) as fuels. The intense electromagnetic field trapped inside the soliton significantly enhances the DT-fusion cross section, its ponderomotive potential evacuates electrons, and it accelerates D/T to kinetic energies suitable for fusion reaction. While electrons are expelled almost instantly, the much heavier D/T moves at picosecond time scale. Such a difference in time scales renders a time window for DT fusion to occur efficiently in an electron-free environment. We inject two consecutive lasers, where the first would excite plasma solitons and the second, much more intense and with a matched lower frequency, would fortify the soliton electromagnetic field resonantly. We impose a plasma density gradient to induce soliton motion. All D/T inside the plasma column swept by the moving soliton during its lifetime would participate in this fusion mechanism. We show that the breakeven condition is attainable. Invoking fiber laser and the iCAN laser technologies for high repetition rate and high intensity operation, gigawatt output maybe conceivable.

In order to bypass the challenges of mainstream schemes to fusion, nonthermal, ballistic, and transient approaches to fusion have been pursued. However, these approaches face their own challenges. One serious issue is the shortness of the penetration depth of the fusion particles relative to their mean free path inside the target because of the smallness of the fusion cross section and the severe energy loss through collisions with the intervening electrons.

It happens that a slowly moving laser-induced plasma soliton can address all these drawbacks in one stroke. Laser-induced plasma solitons are a fundamental phenomenon in the dynamics of laser-plasma interaction, whose property has been well studied and characterized [1–3]. These solitons naturally occur when the laser-plasma interaction is in the non-linear regime, that is, the laser strength parameter  $a_0 \equiv eE/mc\omega > 1$ , where  $E$  is the electric field and  $\omega$  is the frequency of the laser, and the plasma density slightly undercritical. Laser-plasma solitons are super-stable and can move slowly [4]. One salient character of the laser-plasma soliton is that it retains a significant fraction of the laser EM field, albeit at a somewhat down-shifted frequency. For concreteness, we invoke deuterium-tritium (DT) as fuels.

In our scheme, we do two things to the soliton. One, we fortify the trapped laser field strength by coupling the soliton resonantly with a second laser, where the frequency is matched with that of the trapped field in the soliton. The extremely intense EM field trapped in the soliton built up through this method would significantly

enhance the fusion cross section by orders of magnitude. The difference in the time scales between the evacuation of electrons and the motion of the ions renders a time window where the slowly moving fuel particles inside the soliton would propagate in an electron-free environment without much energy loss and a significant fraction of these fuels would fuse under the embedded ultraintense electromagnetic (EM) field with a much enhanced cross section. This ameliorates the problem of severe energy loss of D/T through collisions with electrons.

Another manipulation of the soliton that we do is to induce its motion by assigning the DT target with a decreasing density, so that the soliton propagates with a velocity that is comparable to that of D and T at a certain desired kinetic energy. Such a moving soliton would propagate through a column of plasma within its lifetime. As the soliton continues to enter an unperturbed region of plasma, the same soliton-plasma dynamics described above would repeat until the soliton uses out most of its electromagnetic energy and decays. Since the propagation distance of the soliton within its lifetime is significantly longer than its size, the motion of the soliton therefore contributes to the increase of fueling D/T particles and thus the fusion energy output per laser cycle.

After detailing some aspects of the underlying laser-plasma soliton dynamics, we will provide a self-consistent *strawman design* based on this concept, supported by 2D3V particle-in-cell (PIC) simulations performed using the EPOCH code [5], as an example to demonstrate that the breakeven condition can be reached. We briefly comment on the possibility of *micro ignition* in our scheme.

## Four key elements

The setup of our scheme is natural and relatively simple. Specifically, our system consists of a mixed deuterium-tritium molecule ( $D_2-T_2$ ) gas target with a

\* [pisinchen@phys.ntu.edu.tw](mailto:pisinchen@phys.ntu.edu.tw)

† [r06222017@ntu.edu.tw](mailto:r06222017@ntu.edu.tw)

‡ [gerard.mourou@polytechnique.edu](mailto:gerard.mourou@polytechnique.edu)

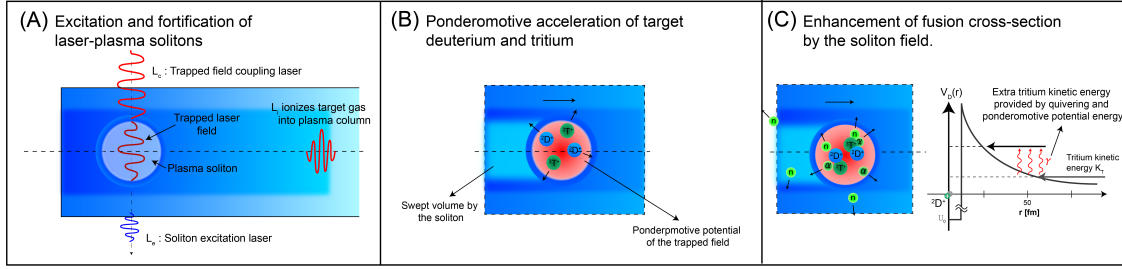


FIG. 1: Four key elements of laser-plasma soliton-enabled fusion: 1. Excitation and fortification of laser-plasma solitons, 2. Ponderomotive acceleration of D/T, 3. Enhancement of fusion cross section by the soliton field, 4. Soliton motion induced by plasma density gradient.

negative density gradient and three laser systems. First, a 800nm *ionization laser*,  $L_i$ , which is used to ionize the gas target into a plasma. Second, an EUV *soliton excitation laser*,  $L_e$ , with  $a_{0,e} > 1$ , and the third, a long-pulse UV *coupling laser*,  $L_c$ , with an ultra-high intensity  $a_{0,c} \gg 1$ , which are injected in sequence in the transverse direction perpendicular to the axis defined by  $L_i$  and the target density gradient, where  $L_e$  induces a chain of  $N$  solitons, followed by  $L_c$  that fortifies the EM field strength of these solitons. We briefly summarize our general concept by breaking it down to four key elements.

1. With the purpose of maximizing the trapped field strength of the soliton in mind, we have discovered a novel mechanism to fortify it (See Appendix A for more details). This is accomplished by injecting a *coupling laser*,  $L_c$ , which follows behind the soliton excitation laser,  $L_e$ , with a proper delay time and with a lower frequency roughly matching that of the trapped laser field in the  $L_e$ -excited soliton,  $\omega_s$ , which in our case is about 1/6 of that of the excitation laser,  $\omega_{0,e}$ . We therefore assign the frequency of  $L_c$  as  $\omega_{0,c} \sim \omega_s \sim 1/6\omega_{0,e}$ . We found that such a matching provides a highly efficient *resonant coupling* (See Appendix B). Figure 2 shows  $a_1$  as a function of the strength parameter  $a_{0,c}$  of  $L_c$ . We see that the fortification of the soliton laser field scales roughly linearly with the strength of the coupling laser  $L_c$ , that is,

$$a_1 \simeq \frac{5}{6} a_{0,c}. \quad (1)$$

2. The ponderomotive potential energy experienced by the ions inside the soliton can be expressed as

$$U_{p,i} = \frac{e^2 E^2}{4m_i \omega_0^2} = \frac{1}{4} \frac{m_e}{m_i} a_1^2 m_e c^2 \simeq \frac{1}{8} \frac{m_e}{m_i} a_1^2 \text{MeV}, \quad (2)$$

where  $m_i = m_D$  and  $m_T$  for deuterium and tritium, respectively. Since the trapped field of the soliton is super-intense ( $a_1 > 100$ ) in our concept, the ions inside the soliton can easily obtain a kinetic energy higher than 10–100 keV, which is suitable for fusion reactions.

3. Laser enhancement of the fusion cross section resorts to lowering the Coulomb potential barrier between

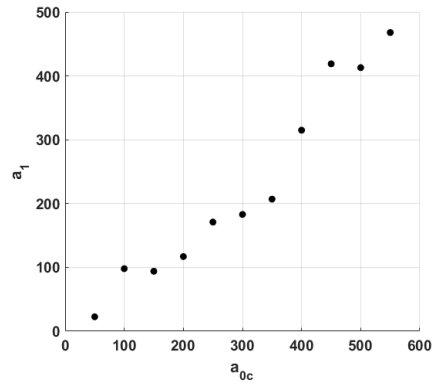


FIG. 2: Dependence of the fortified strength parameter of the soliton laser field,  $a_1$ , on the strength parameter  $a_{0,c}$  of the coupling laser,  $L_c$ .

the fusion particles via laser fields, thereby increasing the transparency and, in turn, the fusion cross section [6, 7]. Figure 3 shows the DT fusion cross section enhanced by the trapped laser field in the soliton as a function of the field strength parameter  $a_1$ . We see that for  $a_1 = 800$ , the fusion cross section is enhanced by a factor  $10^4 - 10^2$  to  $1000 - 500$ barn for colliding deuterium-tritium with center-of-mass kinetic energy  $10 - 50$ keV.

The fusion cross section is often expressed in the well-known Gamow formula,

$$\sigma(\mathcal{E}) = \frac{1}{\mathcal{E}} S(\mathcal{E}) \mathcal{T}(\mathcal{E}), \quad (3)$$

where  $\mathcal{E}$  is the center-of-mass energy of the fusion particles,  $S(\mathcal{E})$  the astrophysical factor, and  $\mathcal{T}(\mathcal{E})$  the Gamow factor, with

$$\mathcal{T}(\mathcal{E}) = e^{-\mathcal{G}/\sqrt{\mathcal{E}}} = e^{-0.011\sqrt{1.7\text{GeV}/\mathcal{E}}} \quad (4)$$

for DT fusion. Since the expression for the DT fusion cross section under an intense laser field is rather complicated, here we deduce a simple empirical formula for the DT fusion cross section that fits all the curves in Fig.3 within the range of the center-of-mass energy

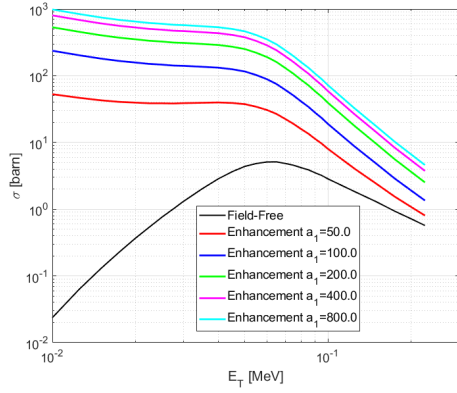


FIG. 3: DT fusion cross section enhanced by trapped laser field in the soliton as a function of field strength parameter  $a_1$ . The black curve represents the baseline scenario, while the other curves represent the enhanced cross section under different soliton field strengths.

$\mathcal{E} \in [0.01, 0.05]\text{MeV}$  and with the soliton EM field ponderomotive energy  $U_p$  much larger than both  $\mathcal{E}$  and the quivering energy  $U_q$ . We find

$$\sigma_{DT}(\mathcal{E}, a_1) \simeq \frac{120}{\sqrt{\mathcal{E}[\text{MeV}]}} e^{-150/a_1} \text{barn}, \quad (5)$$

for energy  $\mathcal{E} \in [0.01, 0.05]\text{MeV}$ .

4. The fourth key element of our concept is inducing motion of the soliton. We have performed a series of 2D Particle-in-Cell (PIC) simulations to investigate the dependence of soliton motion and lifetime on laser and plasma parameters. We found that the soliton velocity is linearly proportional to both the laser strength and plasma the density gradient ( $\propto 1/D_1$ ). We found that the faster the soliton moves, the higher its decay rate and shorter its lifetime, i.e.,  $\tau_s v_s = \text{const.}$  (See Appendix C). For example, based on Eq.(B2), with  $a_1 = 800$  and  $\beta_s = 0.0033$ , the lifetime of the soliton is  $\tau_s = 242\text{psec}$ .

#### Breakeven condition

In our scheme, the breakeven condition corresponds to having the gain factor  $G = \Sigma_n G_n = \Sigma_n \mathcal{E}_{fn}/(\mathcal{E}_i + \mathcal{E}_e + \mathcal{E}_c) \geq 1$ , where  $n = 1, \dots, N$  and  $\mathcal{E}_{fi}$  is the output energy of fusion from the  $i$ th soliton per tri-laser cycle, and the input energy is contributed from the sum of the three lasers:  $L_i, L_e, L_c$ . We will see later that  $\mathcal{E}_i + \mathcal{E}_e \ll \mathcal{E}_c$ . So we can safely ignore the first two terms in the denominator. In terms of fusion output, an intense laser can typically excite multiple solitons ( $N > 1$ ). We focus on the output of the first soliton only and treat that from the remaining solitons as a bonus. Therefore,  $G > G_1 \simeq \mathcal{E}_{f1}/\mathcal{E}_c$ .

The energy of the coupling laser is defined as

$$\mathcal{E}_c = \frac{E_c^2}{8\pi} V_c = \frac{\pi a_{0,c}^2 m_e c^2}{2r_e \lambda_c^2} \left( \frac{4\pi}{3} r_c^2 \tau_c c \right) \simeq \frac{2\pi^2}{3} \frac{\tau_c c}{r_e} a_{0,c}^2 m_e c^2, \quad (6)$$

where  $V_c$  is the volume and  $a_{0,c}$  is the strength parameter of the coupling laser,  $\lambda_c$  is its wavelength,  $r_c$  the transverse size and  $\tau_c$  the pulse duration. Here we choose  $r_c \simeq \lambda_c$  so that the transverse sizes of  $L_e$  and  $L_c$  are roughly matched.

On the other hand, the fusion output energy is

$$\mathcal{E}_{f1} = \eta_s N_{DT} P_{DT} \epsilon_{DT}, \quad (7)$$

where  $\eta_s$  is the efficiency factor that takes into account the erosion of the intensity of the soliton during propagation and  $\epsilon_{DT} = 17.6\text{MeV}$  is the energy released per DT fusion.  $N_{DT}$  is the total number of D and T fuels within the plasma column swept by the propagating soliton with velocity  $v_s$  within its lifetime  $\tau_s$ , that is,

$$N_{DT} = n_p V_s = n_p (4\pi \lambda_s^2 \tau_s v_s). \quad (8)$$

The probability of DT fusion that occurs inside the electron-free soliton, based on our empirical scaling law in Eq.(5), is

$$P_{DT} = \sigma_{DT} \lambda_s \rho_{DT} \simeq \frac{120}{\sqrt{\mathcal{E}[\text{MeV}]}} e^{-150/a_1} \lambda_s n_p \times 10^{-24} \text{cm}^2, \quad (9)$$

where  $\lambda_s$  is the wavelength of the trapped laser field as well as the size of the soliton, and  $\mathcal{E}$  is the center-of-mass energy of the colliding deuterium and tritium.

Putting all these together and recalling that  $a_1 \simeq (5/6)a_{0,c}$  according to Eq.(1), we obtain the gain factor in terms of  $a_1$ :

$$G \simeq \frac{b}{\pi} \eta_s n_p^2 \lambda_s^3 \left( \frac{\tau_s v_s}{\tau_c c} \right) \frac{1}{\sqrt{\mathcal{E}[\text{MeV}]}} \frac{e^{-150/a_1}}{a_1^2} \frac{\epsilon_{DT}}{m_e c^2}, \quad (10)$$

where  $b = 1.4 \times 10^{-34} \text{cm}^3$ . At first glance, it seems that the scheme favors smaller values of  $a_1$ , but in fact PIC simulations show that the fortification of  $a_1$  is primarily due the increase of  $\lambda_s (= (mc^2/eE_s)a_1)$ ; the two are roughly linearly related. Therefore, the actual dependence of  $G$  on  $a_1$  is  $G \propto a_1 e^{-150/a_1}$ , in favor of higher values of  $a_1$ .

#### A strawman design

Based on the considerations above, here we provide a zeroth-order, or strawman conceptual design of our fusion scheme, which is represented by the block diagram in Figure 4. PIC simulations indicate that the excitation of solitons and trapping of the laser field are optimal when the ratio of plasma density to laser critical density,  $\phi_0 \equiv n_p/n_c$ , is  $\sim 0.1$ , where the critical density is defined as  $n_c = \pi/(r_e \lambda_s^2)$ , and  $r_e = e^2/m_e c^2 = 2.8 \times 10^{-13} \text{cm}$  is the classical electron radius. Assuming that the density of the deuterium-tritium plasma at the front end of the target is  $n_p = 5 \times 10^{22} \text{cm}^3$  and demanding  $\phi_0 = 0.1$ , we deduce that the wavelength of  $L_e$  should be  $\lambda_e = 47\text{nm}$ . We choose  $a_{0,e} = 8$ , and find the initial value of the trapped field in the first soliton  $a_1 = 2$  when excited by  $L_e$ . Our aim is to achieve  $a_1 = 800$ . To this end, we inject a *coupling laser*  $L_c$  (cf. Fig.1 and Fig.2).

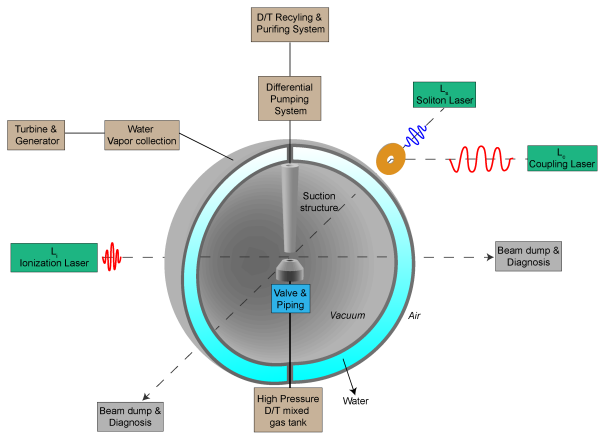


FIG. 4: Block diagram for the laser-plasma soliton DT fusion scheme.

	$\lambda_i$	$a_{0,i}$	Spot size	Pulse duration	Pulse Energy
$L_i$	800nm	1	$2 \times 20\lambda_i$	$40\lambda_i/c$	15mJ
$L_e$	47nm	8	$5\lambda_e$	$5\lambda_e/c$	69mJ
$L_c$	330nm	1000	$1\lambda_c$	$10\lambda_c/c$	572J

TABLE I: Parameters of the three lasers for the DT target density of  $n = 5 \times 10^{22}/\text{cm}^3$ .

Let the transverse spot size of  $L_e$  be  $5\lambda_e$  and the pulse duration  $\tau_e = 5$  laser oscillation cycles, then for a laser strength parameter  $a_{0,e} = eE_s/m_e\omega_e c = 8$ , we find (cf. Eq(6)) the required energy for the soliton excitation laser  $L_e$  is  $\mathcal{E}_e \sim 69\text{mJ}$ .

Next we estimate the energy requirement for the coupling laser  $L_c$ . In order to optimize its coupling with the soliton,  $L_c$  is designed to have a wavelength  $\lambda_c = 330\text{nm}$ , which is about 7 times larger than that of the soliton excitation laser  $L_e$ . Our PIC simulations show that a coupling laser with  $a_{0,c} = 960$  is able to fortify the trapped soliton electromagnetic field strength  $a_1$  from 2 to 800. We match the transverse size of  $L_c$  with that of  $L_e$ , which determines  $r_c = \lambda_c$ . To obtain the desired soliton field, the pulse duration of  $L_c$  is chosen to be 10 cycles. Putting these parameters together, we find  $\mathcal{E}_c = (E_c^2/8\pi)V_c \sim 572\text{J}$ .

Following conventional practice, we invoke  $\lambda_i = 800\text{nm}$  for the ionization laser  $L_i$ , with  $a_{0,i} = 1$ . In order to cover the cross section of multiple solitons, we prepare  $L_i$  with an aspect ratio of the transverse dimensions:  $\sigma_x/\sigma_y = 10$  and  $\sigma_y = 2\lambda_i = 1600\text{nm}$ . The pulse duration of  $L_i$  is limited to single- or few-cycles, say 5, to avoid heating of the plasma. We then find the energy requirement for  $L_i$ ,  $\mathcal{E}_i \sim 15\text{mJ}$ . The parameters of these three lasers are summarized in Table I. As advertised, both  $\mathcal{E}_i$  and  $\mathcal{E}_e < 100\text{mJ} \ll \mathcal{E}_c$ , and they can be safely ignored in the estimate of the gain factor.

Now we envision the gas target density decreases linearly with a gradient  $-3 \times 10^{23}/\text{cm}^4$ . Simulations

indicate that the laser-induced soliton under such a plasma density gradient can propagate with a speed  $v_s \sim 0.0033c$ , which corresponds to the velocity of a tritium with 10 keV kinetic energy.

For a soliton with  $a_1 = 800$ , its ponderomotive potential would induce a maximum kinetic energy,  $\sim 20\text{MeV}$ , to D/T. On the average, however, the kinetic energies of D and T are much lower. Under the plasma density given above and based on Eq.(B2), we find that the maximum soliton lifetime is  $\tau_s \sim 242\text{psec}$ , which translates into a propagation distance of  $\sim 240\mu\text{m}$  in the plasma, within which the change of plasma density is minute.

The size of a laser-plasma soliton is commensurate with the wavelength,  $\lambda_s$ , of the trapped laser field. In our case, with  $a_1 = 800$  and the plasma density  $n_p = 5 \times 10^{22}/\text{cm}^3$ , the wavelength (and the radius) of the soliton is  $\lambda_s \sim 12\mu\text{m} \sim 36\lambda_c$ . With the plasma density  $n_p$  given above, the total number of D and T fuels inside the plasma column swept by the propagating soliton with a velocity  $\beta_s = v_s/c = 0.0033$  within its lifetime  $\tau_s$  is  $N_{\text{DT}} \sim 2.18 \times 10^{16}$  according to Eq(8). The probability of DT fusion that occurs inside the electron-free soliton, based on the cross section given in Fig.3 and choosing  $\mathcal{E} = 0.01\text{MeV}$  as a reference point, and using the empirical fitting formula in Eq.(9), is  $P_{\text{DT}} \sim 0.06$ .

Evidently, the soliton cannot retain the initial value of  $a_1$  during its lifetime as it continues to lose energy. In addition, the plasma density decreases slightly ( $\sim 15\%$ ) over the propagation distance during the lifetime of the soliton. To account for these reductions, we introduce an efficiency factor  $\eta_s \sim 0.5$ . The output energy per tri-laser cycle in our strawman design, based on Eq.(7), is therefore  $\mathcal{E}_{f1} = \eta_s N_{\text{DT}} P_{\text{DT}} \times 17.6\text{MeV} = 1842\text{J}$ .

Putting everything together, we obtain,

$$G = \sum_{n=1}^N G_n > G_1 \simeq \frac{\mathcal{E}_{f1}}{\mathcal{E}_c} \sim 3.2 > 1, \quad (11)$$

which shows that the breakeven condition is in principle attainable in our fusion scheme. We emphasize that this strawman design is not optimized.

In our strawman design the probability of DT fusion is  $P_{\text{DT}} = \sigma_{\text{DT}} \lambda_s \rho_{\text{DT}} \sim 0.06$ , which is already close to unity. One may naturally wonder whether it is possible to exhaust all DT fuel particles, resulting in a *micro ignition*. We hope that by further optimizing the parameters of  $\sigma_{\text{DT}}$ ,  $\lambda_s$ , or  $\rho_{\text{DT}}$ , chain reactions of DT fusion can occur inside the soliton, resulting in a micro ignition.

Both the high intensity EUV  $L_e$  laser and the extremely high power  $L_c$  laser invoked in our fusion scheme are not conventional and would require major R&D. In our strawman design, the output energy per tri-laser cycle is  $\mathcal{O}(\text{kJ})$ . With practical utility in mind, it would be highly desirable to operate the scheme with high repetition rates, such as megahertz, so as to reach GW-level output.

We note that fiber lasers are already capable of delivering MHz repetition rates [8] in routine operation, albeit

with low peak power. On the other hand, the ICAN (International Coherent Amplification Network) consortium [9], which invokes fiber lasers in a coherent manner, has been aiming to develop laser systems that would deliver  $> 10\text{J}$  energy per pulse, with  $> 10\text{kHz}$  repetition rate, and 100–200 femtosecond pulse duration. It is hoped that fiber-laser-based high-intensity, high-repetition-rate lasers will be developed in the near future. By then this laser-plasma soliton DT fusion scheme would become closer to practical applications.

This work is supported by Leung Center for Cosmology and Particle Astrophysics (LeCosPA), National Taiwan University.

#### Appendix A: Fortification of soliton field by a coupling laser

The effect of this enhancement pulse is illustrated in Fig. 5. Without the coupling laser pulse (Fig. 5a), a train of low-amplitude solitons is excited. With the coupling pulse (Fig. 5b), these structures are amplified and merged, resulting in fewer, but substantially more intense and larger solitons.

#### Appendix B: Resonant laser-soliton coupling

The resonant nature of this interaction is confirmed by scanning the wavelength of the coupling laser,  $\lambda_c$ . Figure 6a demonstrates that the final soliton amplitude  $a_1$  exhibits a peak when the ratio of the wavelengths  $\lambda_c/\lambda_e \approx 6$ , highlighting optimal energy coupling. This resonant amplification fundamentally alters the field scaling, which allows for the generation of extreme fields within the soliton from a comparatively modest enhancement pulse.

Such amplification is accompanied by a further red-shifting of the trapped field's frequency. Figure 6b shows a strong positive correlation between the amplified  $a_1$  and the period of the trapped field,  $T_{sol}$ . This frequency down-shift also explains the observed increase in soliton size. Since the soliton radius,  $r_s$ , is fundamentally linked to the trapped wavelength ( $r_s \propto \lambda_s$ ), a larger  $\lambda_s$  results in a larger soliton volume, which is highly advantageous for achieving fusion breakeven condition.

#### Appendix C: Soliton motion and lifetime

Figure 7 shows the soliton velocity as a function of the normalized laser vector potential,  $a_1$ , for various plasma density gradients. For these simulations, a linear down-ramp density profile was employed, characterized by a scale length  $D_1$ , which represents the distance over which the density decreases from its peak value to zero.

A detailed derivation of the exact scaling law and the underlying dynamics is beyond the scope of this paper. Instead, our objective here is to utilize these empirical results to estimate the appropriate parameters for our design. The scaling can be approximated by the relation  $v_s \propto a_1/|\partial n/\partial x|^2$ . Based on Fig. 6, a velocity of  $v_s \approx 0.008c$  can be induced with  $a_1 = 16$  and  $D_1 = 20\text{ }\mu\text{m}$ . Soliton velocities with higher values of  $a_1$  and  $D_1$  can be extrapolated.

The stability of a laser-plasma soliton is due to the balance between the ponderomotive force and the plasma pressure. Since a propagating soliton would continue to enter regions of unperturbed plasma, its ponderomotive energy is consumed to expel electrons and D/T in the newly encompassed region, and therefore loses its energy. This is the dominant mechanism of soliton energy loss. Ignoring other energy-loss effects, the conservation of energy dictates that the soliton decays when it uses out the ponderomotive energy. Therefore, the faster the soliton moves, the higher its decay rate and shorter its lifetime, i.e.,  $\tau_s v_s = \text{const.}$

Since the ponderomotive energy is proportional to  $a_1^2$ , conservation of energy dictates that

$$\frac{da_1^2}{dt} = \alpha \beta_s, \quad (\text{C1})$$

where  $\alpha$  is a proportional constant in units of 1/time and  $\beta_s = v_s/c$ . Figure 6 shows the PIC simulation result that confirms the linear relation between the decay rate and the velocity, from which we deduce  $\alpha = 0.98 \times 10^6[\text{fsec}] \simeq 1 \times 10^6[\text{fsec}]$ . The lifetime of the soliton is therefore,

$$\tau_s = - \int_{a_1}^0 \frac{1}{da_1^2/dt} da_1 = \frac{a_1}{\alpha \beta_s}. \quad (\text{C2})$$

For example, with  $a_1 = 800$  and  $\beta_s = 0.0033$ , the lifetime of the soliton is  $\tau_s = 242\text{ psec}$ .

---

[1] V. Kozlov, A. Litvak, and E. Suvorov, Envelope solitons of relativistic strong electromagnetic waves, Sov. Phys. JETP **49**, 75 (1979).

[2] S. Bulanov, M. Lontano, and P. Sasorov, Ionization rate in the presence of runaway electrons, Physics of Plasmas **4**, 931 (1997).

[3] D. Farina and S. Bulanov, Slow electromagnetic solitons in electron-ion plasmas, Plasma Physics Reports **27**, 641 (2001).

[4] L. Hadzievski, A. Mancic, and M. Skoric, Dynamics of weakly relativistic electromagnetic solitons in laser plasmas, Publications of the Astronomical Observatory of Belgrade **82**, 101 (2007).

[5] T. D. Arber, K. Bennett, C. S. Brady, A. Lawrence-Douglas, M. G. Ramsay, N. J. Sircombe, P. Gillies, R. G. Evans, H. Schmitz, A. R. Bell, and C. P. Ridgers, Contemporary particle-in-cell approach to laser-plasma modelling, Plasma Physics and Controlled Fusion **57**, 1 (2015).

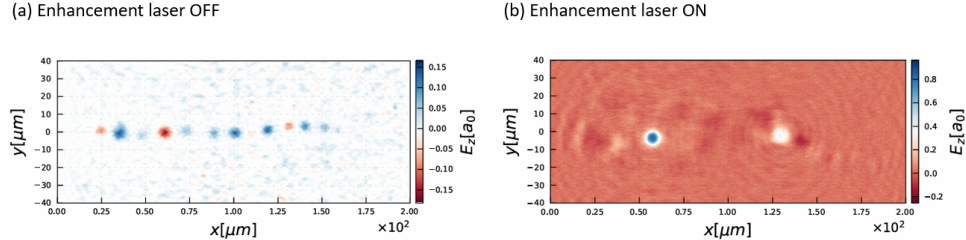


FIG. 5: Fortification of laser-plasma solitons by a coupling pulse. Snapshots of the electric field with same polarization of the incident laser,  $E_z$ , from PIC simulations. (a) A train of low-amplitude solitons generated by a single soliton excitation laser pulse. (b) With the addition of a second, longer-wavelength ‘coupling’ laser, the solitons are amplified and merged, resulting in fewer, larger, and significantly more intense structures. Note the order-of-magnitude increase in the trapped field strength.

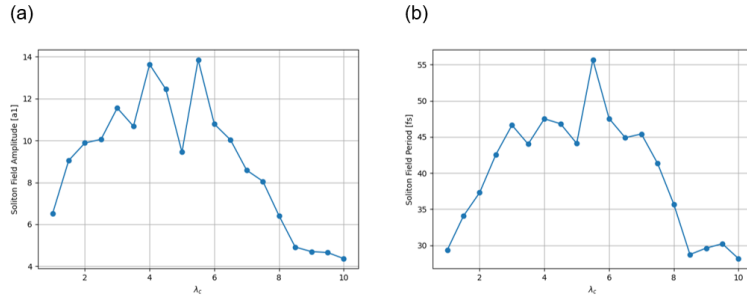


FIG. 6: Resonant amplification of soliton fields. (a) The trapped field amplitude,  $a_1$ , as a function of the coupling laser’s wavelength ratio,  $\lambda_c/\lambda_e$ . A resonance peak is observed around  $\lambda_c/\lambda_e \approx 6$ , indicating the optimal condition for energy coupling. (b) The strong correlation between field amplitude and period confirms that the amplification is accompanied by a significant frequency down-shift of the trapped light.

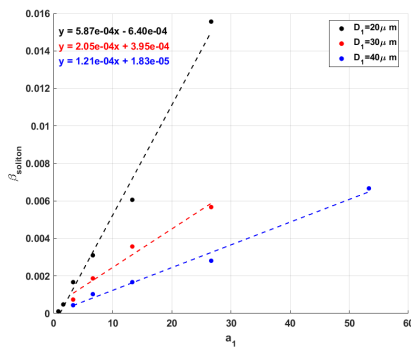


FIG. 7: Soliton velocity  $\beta_s = v_s/c$  as a function of its field strength  $a_1$  for different plasma density gradient scale lengths  $D_1$ . The points represent data from 2D PIC simulations, and the dashed lines are linear fits.

- [6] W. Lv, H. Duan, and J. Liu, Enhanced proton-boron nuclear fusion cross sections in intense high-frequency laser fields, *Nuclear Physics A* **1025**, 122490 (2022).
- [7] M. L. Lindsey, J. J. Bekx, K.-G. Schlesinger, and S. H. Glenzer, Dynamically assisted nuclear fusion in the strong-

field regime, *Physical Review C* **109**, 044605 (2024).

[8] S. D. Chowdhury, S. Manna, S. Chatterjee, R. Sen,

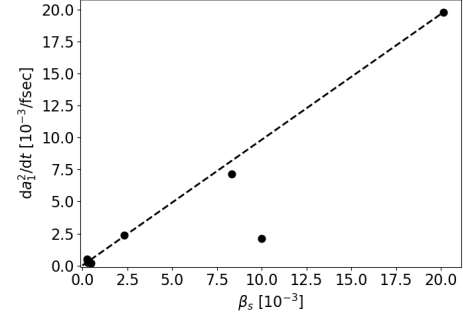


FIG. 8: Soliton lifetime-velocity relation. For a given initial value of the trapped field strength  $a_1$ , the decay rate of a soliton is linearly proportional to its velocity.

and M. Pal, Mega-hertz repetition rate broadband nanosecond pulses from an actively mode-locked yb-fiber laser, *Laser Physics* **29**, 035102 (2019).

- [9] G. Mourou, B. Brocklesby, T. Tajima, and J. Limpert, The future is fibre accelerators, *Nature Photonics* **7**, 258 (2013).